Rapid Communications | Editors' Suggestion

Large tunneling anisotropic magnetoresistance mediated by surface states

Marie Hervé,[1] Timofey Balashov,[1] Arthur Ernst,[2,3] and Wulf Wulfhekel[1]
[1]*Physikalisches Institut, Karlsruhe Institute of Technology, Wolfgang-Gaede-Straße 1, D-76131 Karlsruhe, Germany*
[2]*Institute for Theoretical Physics, Johannes Keppler University Linz, Altenberger Straße 69, A-4040 Linz, Austria*
[3]*Max-Planck-Institut für Mikrostrukturphysik, Weinberg 2, D-06120 Halle, Germany*

(Received 6 January 2018; published 27 June 2018)

We investigate the tunneling anisotropic magnetoresistance (TAMR) in thick hcp Co films at cryogenic temperatures using scanning tunneling microscopy. At around −350 mV, a strong TAMR up to 30% is found with a characteristic voltage dependence and a reversal of sign. With the help of *ab initio* calculations, the TAMR can be traced back to a spin-polarized occupied surface state that experiences a strong spin-orbit interaction leading to a magnetization direction depending on hybridization with bulk states.

DOI: 10.1103/PhysRevB.97.220406

Due to its potential for magnetic storage applications, the tunneling anisotropic magnetoresistance (TAMR) effect has attracted a lot of attention since its discovery [1–6]. It is caused by changes in the tunneling density of states (DOS) with the magnetization direction in heterostructures such as ferromagnet/insulator/normal metal junctions. It originates from spin-orbit coupling (SOC), which lifts the degeneracy of electronic states of a system depending on the magnetization direction. In the case of an out-of-plane TAMR, a magnetic electrode with in-plane and out-of-plane magnetization exhibits two distinct tunneling DOS [7]. It can be produced by the Bychkov-Rashba/Dresselhaus SOC field [7–9] or by a change in the electronic DOS due to SOC-induced band splitting [1]. The TAMR effect was reported for a large spectrum of magnetic films. For example, diluted magnetic semiconductors such as GaMnAs [2–6] display a sizable TAMR. Due to the lack of inversion symmetry in the zinc-blende crystalline structure of GaMnAs, the Dresselhaus effect combined with the Bychkov-Rashba effect at the interfaces produces a TAMR of the order of a few percent. Electronic states of magnetic $3d$ metals hybridized with those of $5d$ transition metals at the interfaces (Fe/W [1], Co/Pt [10,11]) constitute a second class of materials where TAMR effects up to 10% were reported. Recently, a sizable TAMR effect of 10% was reported for a simple fcc Co film epitaxially grown on a sapphire substrate without the help of $3d/5d$ interfaces [12]. In this case, the uniaxial epitaxial strain induces a SOC in combination with a Bychkov-Rashba effect and causes a large TAMR [13].

In order to further increase the TAMR, it was theoretically proposed to use enhanced SOC in spin-polarized surface states at the metallic surfaces and interfaces [14,15]. Indeed, due to a large potential gradient, the Rashba effect can increase at the surfaces and interfaces and can strongly affect the electronic band structure. Depending on the magnetization direction, surface states can hybridize with bulk states and give rise to surface resonances that can produce a sizable TAMR. A TAMR of 20% was theoretically predicted in a Fe/vacuum/Cu junction [14]. Later, a similar proposition was given for Fe/MgO/Fe magnetic tunnel junctions [15], where spin-polarized interface resonances are present [16,17]. The advantage of this approach is the strong momentum selectivity of tunneling across the MgO barrier that can reduce the number of states contributing to tunneling. An experimental observation, however, revealed a TAMR of only ≈1% in the Fe/MgO/Fe junctions [18]. In a photoemission experiment [19], it was shown that bulk states of an Fe thick film near the surface can be influenced by SOC. The authors, however, concludes "in a theoretical study of the TAMR effect in Fe(001) [14], the resonant surface bands (not observed in our experiment) were shown to depend on the magnetization direction, which was also attributed to the Rashba effect."

In this Rapid Communication, we report TAMR effect in hcp Co films of the order of 30% without the need for heavy elements. It is caused by magnetization-direction-dependent hybridization of spin-polarized surface states with bulk bands. We argue that this effect is due to the bulk band structure of Co, and as a consequence shows up in many Co film systems suitable for application.

Co films were grown by molecular beam epitaxy from high-purity Co rods onto clean Ru(0001) surfaces. Details on the substrate preparation can be found elsewhere [20]. After a deposition of 10 monolayers (ML), the sample was annealed to ≈450 °C, which leads to partial dewetting of the film and the formation of flat islands of typically about 30 ML local thickness [21]. Figure 1(a) shows a typical topographic scanning tunneling microscopy (STM) image of the surface. The line scan [Fig. 1(b)] displays a general tilt of the surface due to an unavoidable miscut of the Ru substrate. The Co islands, however, locally form atomically flat terraces. As it has been reported before, Co grows in its hcp modification on Ru(0001) [22].

Figure 1(c) shows a large area map of the differential conductance dI/dU of the sample taken with a nonmagnetic W tip at a bias voltage $U = -330$ mV. A strong contrast is found between the thick hcp Co islands (bright) and the remaining thin wetting layer (dark) due to a large difference in their electronic structure. Further, a clear contrast can be resolved on the Co islands. On the islands, white lines are found that either are closed loops or end at the edges of the islands. Applying an out-of-plane magnetic field leads to a movement of these white

 ©2018 American Physical Society

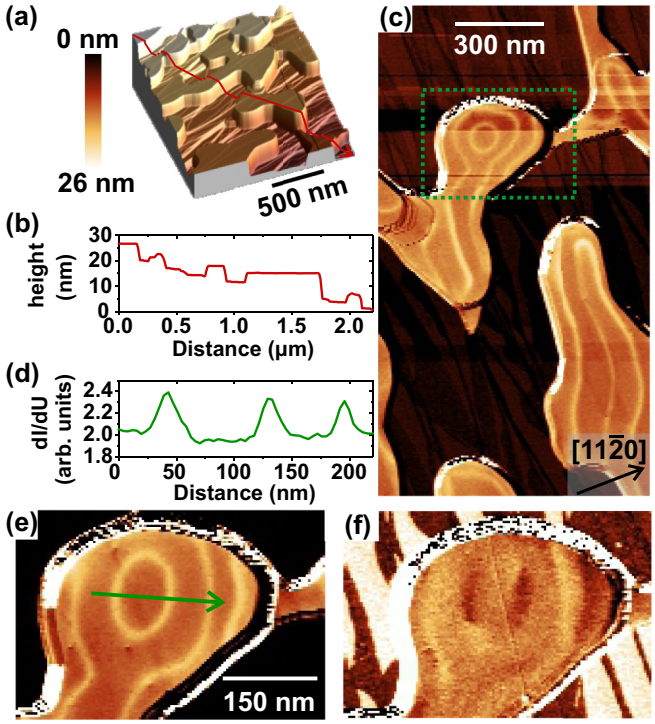

FIG. 1. (a) Large-scale topographic STM image of 10 ML of Co deposited on Ru(0001) postannealed at ≈450 °C ($I = 1$ nA, $U = -330$ mV). (b) Line scan across the structure showing flat island surfaces and the general tilt of the Ru substrate. The typical local Co thickness is about 30 ML. (c) Map of the dI/dU signal showing a domain wall contrast ($I = 1$ nA, $U = -330$ mV, $\Delta U_{\mathrm{rms}} = 30$ mV). (e) Zoomed image and (d) line scan of the area marked by a green dotted box of (c). (f) Spin-polarized dI/dU map recorded with a Co tip of in-plane spin polarization ($I = 1$ nA, $U = -520$ mV, $\Delta U_{\mathrm{rms}} = 50$ mV).

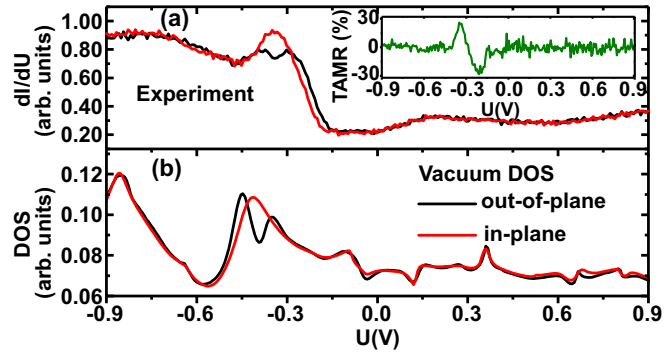

FIG. 2. (a) Voltage dependence of the dI/dU signal recorded with an unpolarized tip on in-plane magnetized domain walls (red) and on out-of-plane magnetized domains (black) displaying a sizable TAMR at ≈ −350 mV (the tip was stabilized at $I = 1$ nA, $U = -1$ V, $\Delta U_{\mathrm{rms}} = 20$ mV). The inset shows a TAMR of up to ±30%. (b) Calculated DOS in the vacuum 0.3 nm in front of the surface. The color scheme is the same as for (a). While for most of the voltages, a sizable TAMR is absent, a characteristic dependence of the DOS is found near −350 mV, in agreement with experiment.

lines (see Supplemental Material Fig. S1 [23]) identifying them as magnetic domain walls. Cobalt in its hcp modification displays a strong uniaxial magnetic anisotropy of about 60% of the dipolar energy with an easy axis along the c axis of the hcp cell [24]. Thus, the Co film in this thickness range forms a magnetic stripe domain pattern [24], in which the out-of-plane magnetocrystalline anisotropy orients the local magnetization normal to the surface plane, i.e., the magnetization points out of or into the plane of the surface. The islands split into magnetic domains in the form of a stripe domain pattern in order to reduce the dipolar energy [24]. Figure 1(d) shows a line scan across a zoomed part of the sample displayed in Fig. 1(e). As can be seen, the dI/dU signal on neighboring domains is identical and only the domain walls appear to be bright. This excludes the tunneling magnetoresistance (TMR) effect as a cause for the observed signal, in agreement with the nonmagnetic tip. Thus, the signal does not depend on the sign of the magnetization but only on its orientation, i.e., out of plane (dark) on the domains and in plane (bright) on the domain walls. It is thus in accord with a TAMR signal. When dipping the W tip into a thick Co island, magnetic Co can be transferred to the tip and the differential conductance then becomes sensitive to the relative orientation of the local sample magnetization and the tip magnetization due to the TMR effect [25,26]. As illustrated in Fig. 1(f), this considerably changes the observed contrast. In this case, the tip became sensitive to the in-plane component of the sample magnetization, and thus the domain walls either appear as bright or dark lines, depending on the direction of magnetization in the walls. Most likely, the walls are of Bloch type due to the large Co thickness [24].

Since the TAMR effect is evoked by a spin-orbit interaction causing modifications in the DOS upon changes in the magnetization axis, it is usually very dependent on the bias voltage. In order to study the bias dependence, we recorded the differential conductance dI/dU on stripe domains with magnetization out of the plane and domain walls with an in-plane magnetization as a function of the bias voltage. Figure 2(a) shows the result in a wide voltage range between −900 and 900 mV. At most bias voltages, dI/dU is identical on the differently oriented magnetic structures. Clear differences only appear near −350 mV, where on the domain walls a broad peak is observed (red curve), while on the domains a double-peak structure with a local minimum at that voltage is seen (black curve). Note that at this bias voltage, a van Hove singularity of an occupied minority surface state of Co has been reported for bulk Co and thin Co films [27–30]. The inset of the figure shows the TAMR, i.e., the difference in the two dI/dU signals over the out-of-plane signal (green curve), which quantifies the TAMR effect. It clearly shows a resonance behavior around −350 mV with a dip slightly below −350 mV, and a peak above. The TAMR is surprisingly large with up to 30%. Note that a similar TAMR is even seen on a single monolayer of Co on Ru(0001), but with a lower amplitude [20].

In order to understand the origin of the TAMR, we carried out first-principles calculations using a full potential relativistic Green's function method, especially designed for semi-infinite systems such as surfaces and interfaces [31,32]. The calculations were performed within the density functional theory in a generalized gradient approximation [33]. The dI/dU signals were simulated within the Tersoff-Hamann approximation, in

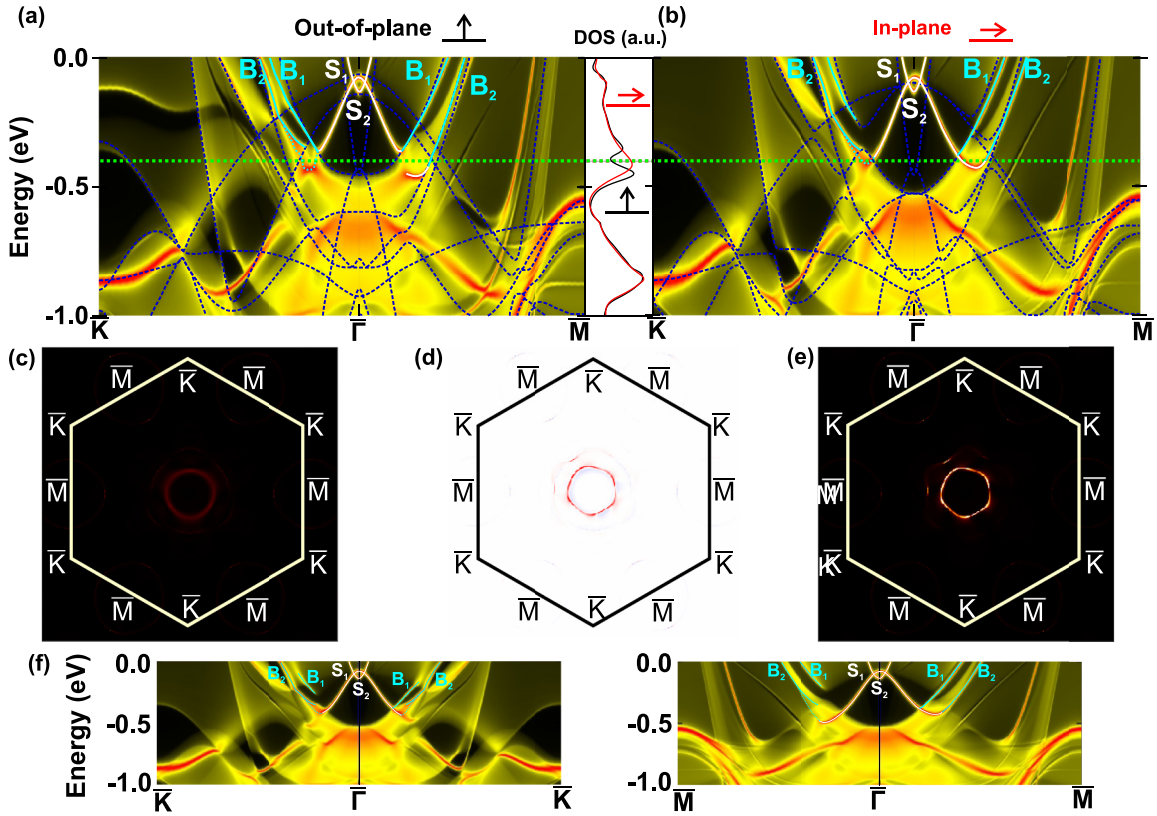

FIG. 3. (a), (b) Band structure of bulk Co (dashed dark blue lines) and the surface (yellow/red) for out-of-plane and in-plane magnetization, respectively. The surface and surface/bulk hybridized state are marked by white and light blue lines, respectively. For comparison, the DOS of Fig. 2 has been repeated between the panels. (c), (e) k-resolved vacuum DOS at -400 mV in the 2D surface Brillouin zone for out-of-plane and in-plane magnetization, respectively, using the same color scale. (d) Changes in the k-resolved density of states upon rotation of the magnetization. (f) Dispersion of the surface states for an in-plane magnetization along inequivalent directions in the surface Brillouin zone.

which a dI/dU signal is associated with the local density of states (LDOS) calculated in vacuum at a certain distance from the surface [34]. In our study we calculated the LDOS at 3.5 Å above the surface.

The calculated LDOS [Fig. 2(b)] qualitatively reproduces the measured dI/dU signal. The overall shape of the LDOS agrees with the experimental data. Especially, it shows nearly identical LDOS for both magnetic configurations at most of the energies, i.e., an absence of a TAMR effect. Only near -350 mV does the LDOS significantly depend on the orientation axis of the magnetization. The calculated LDOS nicely reflects the single-peak structure for in-plane magnetization (red) and the double-peak structure for out-of-plane magnetization (black). Note that the calculations show a slightly larger difference than observed in the experiment and also the energies are slightly different. These small deviations from the experiment may either be due to the limits of density functional theory (DFT) or due to the difference of the samples. In the experiments, we deal with Co films of finite thickness on Ru(0001), which may display some strain due to the lattice mismatch to the substrate, while the calculations were carried out for a half-infinite Co structure with its natural lattice constant.

Finally, the DFT calculations allow us to identify the origin of the observed large TAMR effect. Figures 3(a) and 3(c) display the calculated two-dimensional (2D) band structure at the Co surface. Bulk states are superposed as dark blue dashed lines while states only present at the surface are displayed in yellow/red. The intensity in the figure represents the weight of the states on a logarithmic scale. For clarity, the surface and surface/bulk hybridized states discussed in the following are marked by white and light blue lines, respectively. For comparison, the LDOS of Fig. 2(b) is replotted vertically to size next to the band structure. As can be seen, the differences in LDOS around -350 mV are caused by large changes in the surface band structure and are related to a forbidden band crossing. In the following, we analyze the band structure in more detail. As can be seen from Figs. 3(a) and 3(b), the unoccupied surface state of positive effective mass S_1 near the $\bar{\Gamma}$ point is not affected by changes of the magnetization axis and is not involved in the TAMR. Several of the bulk bands, which cross in the case of an out-of-plane magnetization, develop forbidden crossings when the magnetization is rotated into the plane. This, however, hardly affects the LDOS of the bulk (see Supplemental Material Fig. S2 [23]). The most prominent changes in the surface electronic structure arise from changes in the surface state S_2. The S_2 surface state of negative effective mass is of a minority and $d_{3z^2-r^2}$ character [29,30,35]. For an in-plane magnetization, S_2 merges continuously with the bulk band B_2 causing states with vanishing group velocity and a van Hove singularity near -400 meV. Figure 3(e) displays a two-dimensional plot of the states in the surface Brillouin zone and shows a bright ring at that energy as a consequence

(plotted on a linear scale). For an out-of-plane magnetization, S_2 hybridizes with B_1 and develops a gap near -400 meV, reducing the density of states in the two-dimensional Brillouin zone at that energy [compare Fig. 3(c)]. This gap is responsible for the reduction of the DOS at -400 meV and causes the TAMR. Its spectral weight is shifted away from the gap and causes the double-peak feature in the DOS. This is further illustrated by the change of the DOS depicted in Fig. 3(d) plotted in a linear scale (red for a reduction and blue for an increase). Note that B_1 has a large weight of $J = 5/2$, $J_z = -5/2$ so that it can hybridize well with S_2 of the same character for an out-of-plane magnetization, while B_2 is more of a $J = 3/2$ character. When the magnetization is turned in the plane, however, the spin states of all bands become a coherent superposition of the two spin directions and the Clebsch-Gordan coefficients now allow hybridization of S_2 and B_1 (for analysis of the character of the bands, see Supplemental Material Fig. S3 [23]). As the phase of the superposition of the spin state depends on the in-plane direction of magnetization, the hybridization is different for different wave vectors $\vec{k}$, as illustrated in Fig. 3(f).

In conclusion, we have shown that simple hcp Co shows a large TAMR of $\pm 30\%$ near -350 mV caused by hybridization of the surface state and the bulk states. Thus, this effect is expected to be rather robust to the details of the Co film. Note that similar surface states have been reported even for 2 ML Co films on Cu(111) and Au(111) of both fcc and hcp stacking [30] and Co on W(110) [35]. As shown recently, a TAMR of 5% at the same energy was found for a single monolayer of Co on Ru(0001) [20], further emphasizing the robustness of this effect, while it is difficult to speak of bulk and surface states in a single monolayer. Moreover, the analysis of the character of the bands allows us to give a general recipe to obtain large TAMR effects at the interfaces and surfaces. The interface or surface state should display a maximal J and J_z (large orbital momentum with an aligned spin) and then can hybridize with bulk $J = 5/2$ or $J = 3/2$ bulk states depending on the orientation of magnetization.

We acknowledge funding by the Deutsche Forschungsgemeinschaft (DFG) under Grant No. WU349/15-1 and through priority program SPP1666 (Topological Insulators), by the European Commission (Grant ATOMS FP7/2007-2013-62260), discussions with B. Dupé and M. Martins, and technical support from J. Chen, M. Peter, and J. Jandke.

[1] M. Bode, S. Heinze, A. Kubetzka, O. Pietzsch, X. Nie, G. Bihlmayer, S. Blügel, and R. Wiesendanger, Phys. Rev. Lett. **89**, 237205 (2002).
[2] C. Gould, C. Rüster, T. Jungwirth, E. Girgis, G. M. Schott, R. Giraud, K. Brunner, G. Schmidt, and L. W. Molenkamp, Phys. Rev. Lett. **93**, 117203 (2004).
[3] C. Rüster, C. Gould, T. Jungwirth, J. Sinova, G. M. Schott, R. Giraud, K. Brunner, G. Schmidt, and L. W. Molenkamp, Phys. Rev. Lett. **94**, 027203 (2005).
[4] A. D. Giddings, M. N. Khalid, T. Jungwirth, J. Wunderlich, S. Yasin, R. P. Campion, K. W. Edmonds, J. Sinova, K. Ito, K.-Y. Wang *et al.*, Phys. Rev. Lett. **94**, 127202 (2005).
[5] H. Saito, S. Yuasa, and K. Ando, Phys. Rev. Lett. **95**, 086604 (2005).
[6] R. Giraud, M. Gryglas, L. Thevenard, A. Lemaître, and G. Faini, Appl. Phys. Lett. **87**, 242505 (2005).
[7] A. Matos-Abiague and J. Fabian, Phys. Rev. B **79**, 155303 (2009).
[8] Y. A. Bychkov and E. I. Rashba, J. Phys. C **17**, 6039 (1984).
[9] G. Dresselhaus, Phys. Rev. **100**, 580 (1955).
[10] B. G. Park, J. Wunderlich, D. A. Williams, S. J. Joo, K. Y. Jung, K. H. Shin, K. Olejník, A. B. Shick, and T. Jungwirth, Phys. Rev. Lett. **100**, 087204 (2008).
[11] A. B. Shick, F. Máca, J. Mašek, and T. Jungwirth, Phys. Rev. B **73**, 024418 (2006).
[12] K. Wang, T. L. A. Tran, P. Brinks, J. G. M. Sanderink, T. Bolhuis, W. G. van der Wiel, and M. P. de Jong, Phys. Rev. B **88**, 054407 (2013).
[13] A. Matos-Abiague, M. Gmitra, and J. Fabian, Phys. Rev. B **80**, 045312 (2009).
[14] A. N. Chantis, K. D. Belashchenko, E. Y. Tsymbal, and M. van Schilfgaarde, Phys. Rev. Lett. **98**, 046601 (2007).
[15] M. N. Khan, J. J. Henk, and P. Bruno, J. Phys.: Condens. Matter **20**, 155208 (2008).
[16] C. Tusche, H. L. Meyerheim, N. Jedrecy, G. Renaud, A. Ernst, J. Henk, P. Bruno, and J. Kirschner, Phys. Rev. Lett. **95**, 176101 (2005).
[17] C. Tiusan, J. Faure-Vincent, C. Bellouard, M. Hehn, E. Jouguelet, and A. Schuhl, Phys. Rev. Lett. **93**, 106602 (2004).
[18] Y. Lu, H.-X. Yang, C. Tiusan, M. Hehn, M. Chshiev, A. Duluard, B. Kierren, G. Lengaigne, D. Lacour, C. Bellouard *et al.*, Phys. Rev. B **86**, 184420 (2012).
[19] E. Młyńczak, M. Eschbach, S. Borek, J. Minár, J. Braun, I. Aguilera, G. Bihlmayer, S. Döring, M. Gehlmann, P. Gospodarič *et al.*, Phys. Rev. X **6**, 041048 (2016).
[20] M. Hervé, B. Dupé, R. Lopes, M. Böttcher, M. D. Martins, T. Balashov, L. Gerhard, J. Sinova, and W. Wulfhekel, Nat. Commun. **9**, 1015 (2018).
[21] C. Yu, J. Pearson, and D. Li, J. Appl. Phys. **91**, 6955 (2002).
[22] F. El Gabali, J. M. Puerta, C. Klein, A. Saa, A. K. Schmid, K. F. McCarty, J. I. Cerda, and J. de la Figuera, New J. Phys. **9**, 80 (2007).
[23] See Supplemental Material at http://link.aps.org/supplemental/10.1103/PhysRevB.97.220406 for further descriptions, and Figs. S1, S2, and S3.
[24] A. Hubert and R. Schäfer, *Magnetic Domains: The Analysis of Magnetic Microstructures* (Springer, Berlin, 1998).
[25] M. Julliere, Phys. Lett. A **54**, 225 (1975).
[26] R. Wiesendanger, Rev. Mod. Phys. **81**, 1495 (2009).
[27] F. J. Himpsel and D. E. Eastman, Phys. Rev. B **20**, 3217 (1979).
[28] L. Diekhöner, M. A. Schneider, A. N. Baranov, V. S. Stepanyuk, P. Bruno, and K. Kern, Phys. Rev. Lett. **90**, 236801 (2003).
[29] M. A. Barral, M. Weissmann, and A. M. Llois, Phys. Rev. B **72**, 125433 (2005).

[30] B. Heinrich, C. Iacovita, M. V. Rastei, L. Limot, P. A. Ignatiev, V. S. Stepanyunk, and J. P. Bucher, Eur. Phys. J. B **75**, 49 (2010).
[31] M. Lüders, A. Ernst, W. M. Temmerman, Z. Szotek, and P. J. Durham, J. Phys.: Condens. Matter **13**, 8587 (2001).
[32] M. Geilhufe, S. Achilles, M. A. Köbis, M. Arnold, I. Mertig, W. Hergert, and A. Ernst, J. Phys.: Condens. Matter **27**, 435202 (2015).
[33] J. P. Perdew, K. Burke, and M. Ernzerhof, Phys. Rev. Lett. **77**, 3865 (1996).
[34] J. Tersoff and D. R. Hamann, Phys. Rev. B **31**, 805 (1985).
[35] J. Wiebe, L. Sacharow, A. Wachowiak, G. Bihlmayer, S. Heinze, S. Blügel, M. Morgenstern, and R. Wiesendanger, Phys. Rev. B **70**, 035404 (2004).